High-Efficiency Triple-Helix-Mediated Photo-Cross-Linking at a Targeted Site within a Selectable Mammalian Gene†

Karen M. Vasquez,‡ Theodore G. Wensel,‡ Michael E. Hogan,§ and John H. Wilson*,‡

Verna and Marrs McLean Department of Biochemistry and Department of Molecular Physiology and Biophysics, Baylor College of Medicine, One Baylor Plaza, Houston, Texas 77030

Received April 12, 1996; Revised Manuscript Received June 17, 1996⊗

ABSTRACT: Targeting damage to specific sites in the genome represents an attractive approach to manipulating gene function in mammalian cells. To test the applicability of triple-helix formation as a means for achieving precisely timed site-specific damage within a mammalian gene, a triplex-forming oligodeoxyribonucleotide (TFO) that binds with high affinity to a specific site within the hamster adenine phosphoribosyltransferase (APRT) gene was modified with the photochemically reactive psoralen derivative 4′-(hydroxymethyl)-4,5′,8-trimethylpsoralen (HMT). The modified TFO, psorTFO1, bound with high affinity to a target site within intron 1 of the APRT gene. Upon irradiation, photomonoadducts (*i.e.*, covalent adducts of psorTFO1 to one strand of the target duplex) were formed with high efficiency (∼50%). Introduction of 5′-TpA sequences (the preferred site for psoralen-induced photo-cross-links) at or near the triplex junction leads to increased efficiency of total photoadduct formation and to efficient formation of products that had the electrophoretic mobility on denaturing PAGE expected for three-stranded photo-cross-links (*i.e.*, products containing psorTFO1 covalently linked to both strands of the duplex). Their identities as cross-links were verified by (1) identical electrophoretic mobility of products formed with either duplex strand radiolabeled and (2) coprecipitation of the radiolabeled duplex strand with its complementary biotinylated strand following denaturation. In addition, the cross-links were completely reversible upon irradiation at 254 nm, as expected for psoralen-mediated cross-links. The yield and distribution of photoadducts depended on 5′-TpA position. The most efficient photoadduct formation (∼90%) and photo-cross-link formation (∼90% of total photoadducts) were observed for a 5′-TpA adjacent to the triplex junction, with significant, but lower, cross-linking efficiency within three base pairs of the junction. Molecular models of the psoralen-conjugated triplex with its six-carbon linker suggested a simple explanation for this distance dependence: facile intercalation near the triplex/duplex junction, with increasing strain required for intercalation at more distant sites. These results indicate that psorTFO1 allows for DNA damage with high precision and high efficiency, and the likely proportion of monoadducts and cross-links can be estimated from the target sequence.

Damage to the mammalian genome can dramatically increase the rates of recombination and mutation (Friedberg et al., 1995). Targeting such damage to specific sites has the potential for controlled gene manipulation, allowing targeted replacement, repair, mutation, or inactivation of specific genes. A promising approach to site-selective DNA damage is the use of modified triplex-forming oligonucleotides (TFOs)[1] designed to bind to unique sites on double-stranded DNA within a mammalian genome. Induction of intracellular triplex formation by extracellular application of TFOs has been successfully used to suppress transcription in cells (Postel et al., 1991; Orson et al., 1991; McShan et al., 1992; Grigoriev et al., 1993; Ing et al., 1993; Okada et al., 1994; Roy, 1994; Scaggiante et al., 1994; Tu et al., 1995; Kovacs et al., 1996), to inhibit replication (Birg et al., 1990), and to induce site-specific mutations in an extrachromosomal vector transfected into mammalian cells (Wang et al., 1995, 1996).

Of the several classes of DNA−DNA triplexes, those formed by GT-rich TFOs (Cooney et al., 1988; Hogan et al., 1989; Beal & Dervan, 1991) bind in the major groove of the underlying duplex in an antiparallel fashion through a reverse Hoogsteen hydrogen-bonding motif and form stable three-stranded DNA complexes at physiological pH. The affinities with which such triplexes form can be quite high; K_d values $< 10^{-9}$ M have been observed, and the mean bound lifetimes for these triplexes can be many hours (Vasquez et al., 1995). In addition, TFOs with a 3′-propanolamine modification, have been shown to be stable *in vivo* for many hours (Zendegui et al., 1992).

Chemical and photochemical DNA damaging agents have been used extensively to study the effects of random DNA damage. Combining the site specificity conferred by triplex formation with temporal control through use of photoactivatable DNA damaging agents attached to TFOs has the potential to optimize site-specific DNA damage without

† This work was funded by grants from the NIH to J.H.W. (GM38219) and M.E.H. (A132804), a grant from the Welch Foundation to T.G.W. (Q1179), a grant to J.H.W. and T.G.W. from the Texas Advanced Technology Program (004949-083), and by Aronex Pharmaceutical Corp.

* Address correspondence to this author. Phone: (713) 798-5760. FAX: (713) 795-5487. email: jwilson@bcm.tmc.edu.

‡ Verna and Marrs McLean Department of Biochemistry.

§ Department of Molecular Physiology and Biophysics.

⊗ Abstract published in *Advance ACS Abstracts,* August 1, 1996.

[1] Abbreviations: APRT, adenine phosphoribosyltransferase; CHO, Chinese hamster ovary; TFO, triplex-forming oligodeoxyribonucleotide; HMT, 4′-(hydroxymethyl)-4,5′,8-trimethylpsoralen; psorTFO1, the conjugate of HMT with the specific TFO targeted to APRT intron 1.

S0006-2960(96)00881-1 CCC: $12.00

detriment to the rest of the genome. Triplex-mediated DNA damage has been used *in vitro* to induce site-specific DNA nicking, cleavage, and cross-linking (Moser & Dervan, 1987; Perrouault et al., 1990; Strobel et al., 1991; Takasugi et al., 1991).

The most widely used class of photoactivatable DNA damaging agents are the psoralens. Various psoralen derivatives have been used extensively in clinical applications and have contributed significantly to our understanding of nucleic acid structure through their ability to intercalate into and covalently photo-cross-link double-stranded nucleic acids (Ben-Hur & Song, 1984). Psoralens are tricyclic, planar molecules, containing a photoreactive furan or pyrone moiety on either side of a benzene ring. Their photochemistry is well characterized (Cimino et al., 1985). For psoralens in general, upon absorption of one photon a covalent monoadduct can be formed with a pyrimidine on one strand of DNA, and if the monoadduct is formed with the furan side, it can be converted to a cross-link by absorption of another photon and reaction with an adjacent pyrimidine in the complementary strand. If the monoadduct occurs on the pyrone side, however, cross-link formation is not possible. The reactivity of psoralen is sequence dependent, and the preferred order is 5′-TpA > 5′-ApT ≫ 5′-TpG > 5′-GpT (Esposito et al., 1988). Psoralen photodamage has been shown to induce intracellular DNA repair machinery (Reardon et al., 1991) and to enhance rates of mutation (Bridges et al., 1979), gene conversion (Averbeck, 1985), and recombination (Cole, 1971; Hall, 1982) with little sequence specificity. Psoralen-conjugated TFOs have been used in cultured mammalian cells to inhibit transcription specifically (Grigoriev et al., 1993; Degols et al., 1994) and enhance site-specific mutation in transiently transfected plasmids (Havre et al., 1993; Havre & Glazer, 1993).

In order to apply this technology to manipulation of specific sites within mammalian chromosomes, we have studied triplex formation within intron 1 of the hamster adenine phosphoribosyltransferase (APRT) gene (Vasquez et al., 1995). This short (2.3 kb) well-characterized gene is subject to both positive and negative selection, and numerous cell lines are available with modified APRT loci designed to facilitate studies of recombination and mutation in a chromosomal context (Sargent et al., 1996). A TFO (TFO1) targeted to the APRT intron 1 site binds with high affinity and specificity and dissociates very slowly once triplex is formed (Vasquez et al., 1995). Here we describe the photoreactions of TFO1 conjugated to 4′-(hydroxymethyl)-4,5′,8-trimethylpsoralen (psorTFO1) with the intron 1 target site and the effects of introducing 5′-TpA sites at strategic positions in the target duplex.

EXPERIMENTAL PROCEDURES

Oligonucleotide Synthesis and Purification. Oligodeoxyribonucleotides were synthesized on an automated MilliGen 8700 DNA synthesizer (Millipore Corp., Milford, MA) using standard solid-phase chemistry and deprotected as previously described (Vasquez et al., 1995) or purchased from Genosys Biotechnologies, Inc. (The Woodlands, TX). All TFOs contained a propanolamine (3′-$OPO_2OCH_2CHOHCH_2NH_3^+$) group on the 3′ end. The concentration of DNA was determined by UV absorbance. Integrity of the oligonucleotides was analyzed by PAGE with oligos 5′-end-labeled using T4 polynucleotide kinase (Boehringer-Mannheim, Indianapolis, IN) and [γ-^{32}P]ATP (6000 Ci/mmol) (New England Nuclear Research Products, Boston, MA). Psoralen-modified TFOs were synthesized on a MilliGen Expediter synthesizer with an extended coupling time of 10 min. The psoralen derivative, (2-[4′-(hydroxymethyl)-4,5′,8-trimethylpsoralen]hexyl-1-*O*-(2-cyanoethyl)-*N*,*N*-diisopropylphosphoramidite), was purchased from Glen Research and was coupled to the 5′ end. Psoralen TFOs were purified by HPLC on a 1 cm × 10 cm column packed with POROS II RP (20 μm), gel purified, and characterized by UV absorbance and fluorescence spectroscopy.

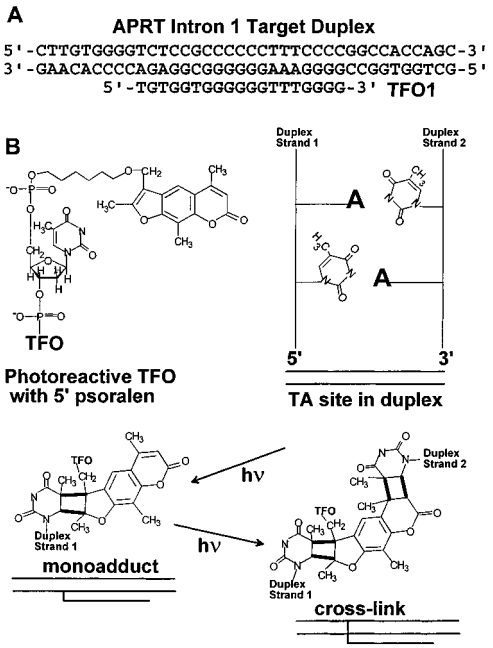

FIGURE 1: Schematic diagram of the native APRT intron 1 site and proposed photochemical reactions with psorTFO1. (A) APRT intron 1 triplex showing the sequences of the duplex target and TFO1. The 38 bp target site duplex spans bases 550−587 of the hamster APRT gene, with the triplex binding site from bp 559−577. (B) Proposed psoralen reaction pathway for a 5′-TpA site. The psoralen-modified TFO is depicted with a 4′-(hydroxymethyl)-4,5′,8-trimethylpsoralen group on the 5′ end.

Triplex Formation. Oligonucleotides corresponding to the sequence surrounding the intron 1 site (Figure 1A; Vasquez et al., 1995) were annealed in a 1:1 molar ratio to form a target duplex, with one strand of the duplex radiolabeled. Single strands were 5′-end-labeled using T4 polynucleotide kinase and [γ-^{32}P]ATP, and following annealing, the duplex was gel purified. Duplex (at 5×10^{-8} M) was incubated for the indicated times with increasing concentrations of TFO in standard triplex buffer (10 mM Tris-HCl, pH 7.6, 1 mM spermine, 10% sucrose, w/v) at 37 °C. To determine strand specificity of photoreactions and to compare mobilities of partially and fully phosphorylated products, duplexes were prepared containing either strand radiolabeled by itself, both strands radiolabeled to high specific activity, or either strand tracer labeled with high specific activity [γ-^{32}P]ATP, followed by exhaustive phosphorylation of both strands with nonradioactive ATP. Triplex formation reactions with the psoralen-modified TFOs were carried out in a dark room, using only dim red illumination from a photographic safe light. Triplex formation was verified by electrophoretic band shift assays as described previously (Vasquez et al., 1995).

Photolysis and Photoadduct Analysis. Following incubation, the samples were irradiated with UVA for the times indicated in the figure legends. The light source used was

a high-intensity (150 W, Oriel) xenon/mercury arc lamp (~12 J/cm^2 per minute of irradiation, based on the manufacturer's specifications) focused on the sample, using a $NaNO_3$ solution filter to eliminate infrared. For the irradiation dose corresponding to a time point of 0.6 s (0.12 J/cm^2), samples were irradiated for 6 s using a 1.0 OD neutral density filter in conjunction with the $NaNO_3$ filter. After irradiation, reaction products were denatured at 97 °C in 50% (v/v) formamide and analyzed by denaturing PAGE. Electrophoresis was through a 7 M urea−15% polyacrylamide gel containing 89 mM Tris, 89 mM boric acid, pH 8.0, and 2 mM EDTA (TBE, unless otherwise noted). Gels were run for 1−2 h at 60 W at 55 °C, dried, and exposed to film for autoradiography. For quantitation, radioactivity was measured using a Betagen Beta Scope 603 blot analyzer. Photoadduct yields for each duplex varied somewhat as a function of lamp configurations and age of psorTFO1 stocks; under Results, both the yields obtained in the experiments shown and the maximum yields obtained are given.

Photoreversibility of Cross-Links. Radiolabeled cross-linked bands were gel purified from a 15% polyacrylamide gel containing 7 M urea. Bands were electroeluted in TBE and concentrated by centrifugal filtration. The purified cross-links were then irradiated at 254 nm using a xenon/mercury arc lamp filtered to select either 254 or 334 nm light only. The reaction products were then subjected to denaturing PAGE on a 15% polyacrylamide gel, which was dried prior to autoradiography.

Verification of Cross-Links. Biotinylated oligonucleotides were purchased from Genosys Biotechnologies, Inc. (The Woodlands, TX). Duplexes were annealed and gel purified with one strand containing 5′-biotin and the complementary strand radiolabeled on the 5′ end. Biotinylated vesicles were made by mixing a solution of 98% phosphatidylcholine with 2% biotin X−dipalmitoylphosphatidylethanolamine (Molecular Probes, Inc., Eugene, OR). The mixture was dried under vacuum and resuspended in TE (10 mM Tris, pH 7.4, 1 mM EDTA). The phospholipid mixture was then extruded ten times through two 0.2 μM polycarbonate filters, using a Lipex extrusion device. TFO (10^{-6} M) was added to target duplex (5×10^{-8} M) in standard triplex binding buffer and incubated for 2 h at 37 °C to allow formation of triplex. Samples were irradiated with UVA (as described above) for 6 s. The reaction products were heat denatured (97 °C, 10 min), and a 50-fold excess of unlabeled strand was added to compete with the labeled strand of the duplex. Streptavidin (50 μg/mL) was added to the sample, and the reaction mixture was vortexed and incubated for 30 min on a shaker at room temperature. Following the incubation period, biotin vesicles were added (350 mM), and the reaction mixture was again vortexed and shaken for 30 min at room temperature. To pellet the vesicles, the samples were centrifuged in an Eppendorf for 20 min, the supernatant was removed, and TE was added to wash the pellet, which was then centrifuged for another 20 min. The supernatant, pellet, and wash fractions either were added to scintillation fluid for radioactivity measurements by scintillation counting or were denatured, phenol/chloroform extracted, and analyzed by denaturing PAGE.

RESULTS

Photoadduct Formation by PsorTFO1 at the Native APRT Intron 1 Site. When psorTFO1 binding to the APRT intron 1 site target duplex was measured using standard band-shift analysis (Vasquez et al., 1995), neither a significant increase nor a decrease in affinity was observed as compared to the unmodified TFO ($K_d \leq 10^{-9}$ M; data not shown). As shown in Figure 2, irradiation of the preformed triplex with ultraviolet light led to fairly efficient formation of photoadducts, as evidenced by the appearance of new species with greatly altered electrophoretic mobility. On the basis of established psoralen photochemistry [*e.g.*, Gasparro et al. (1994)], two types of photoadducts are expected upon irradiation: monoadducts consisting of psorTFO1 covalently linked to one strand of the duplex (either of the complementary strands is a potential target) and cross-links, in which both duplex strands are covalently linked to psorTFO1, resulting in a covalent three-stranded structure (see Figure 1B). The distribution of photoadducts shown in Figure 2 reveals that the major products had electrophoretic mobilities consistent with monoadduct formation. The multiplicity of bands that migrate as monoadducts is not surprising given that each strand of the duplex has a distinct electrophoretic mobility, and there may be more than one site of reaction with psoralen. Quantitation of radioactivity of the products indicated a total photoadduct yield of 42% (±3%) for the experiment shown in Figure 2 (maximum of 55% in all experiments; see Experimental Procedures). Products with sufficiently slow mobility to be cross-links accounted for less than 3% of the total photoadduct radioactivity.

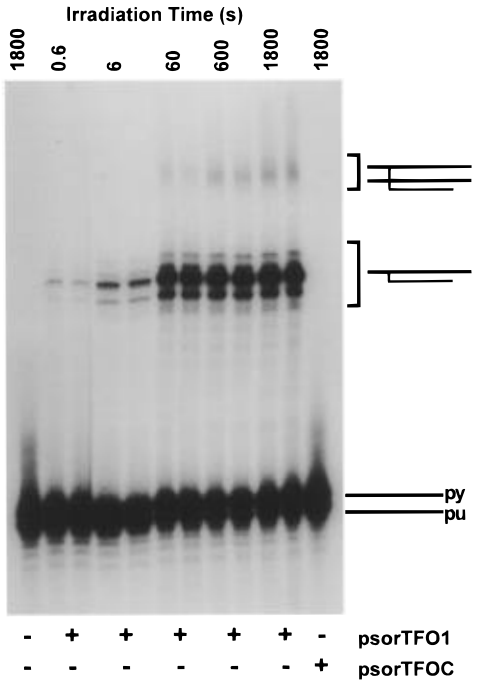

FIGURE 2: Electrophoretic analysis of photoadducts formed by psorTFO1 at the native APRT intron 1 site. End-labeled target duplex (5×10^{-8} M) was incubated for 2 h with either psorTFO1 or a control psoralen TFO (psorTFOC), at a concentration of 1×10^{-6} M in standard triplex binding buffer (see Experimental Procedures). The control oligonucleotide, psorTFOC, has the same base composition as psorTFO1 but a scrambled sequence that does not bind the intron 1 site. The preformed triplex was irradiated for various times, as indicated, using a Xe/Hg arc lamp (12 J/cm^2 per min) and then subjected to denaturing PAGE and autoradiography. Positions on the gel are indicated for the labeled duplex strands and for the photoadducts whose mobilities correspond to monoadducts (two connected lines) or cross-links (three connected lines). The label py stands for pyrimidine-rich strand (top strand in Figure 1A) and pu for purine-rich strand (bottom strand in Figure 1A).

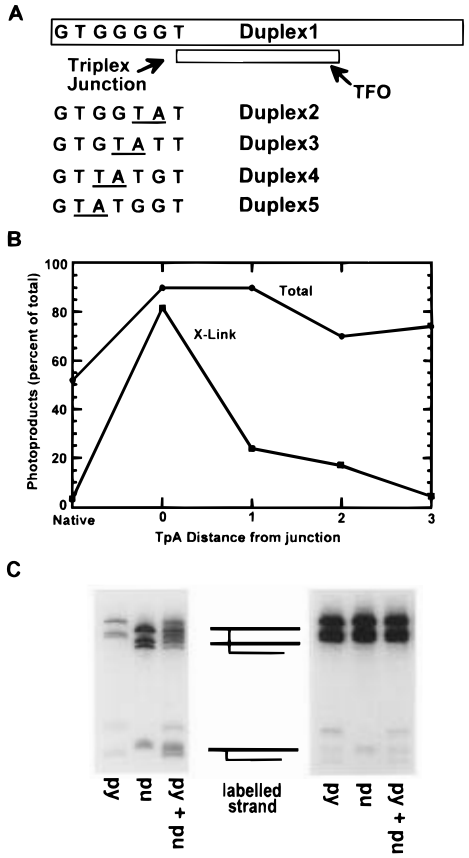

FIGURE 3: Photoreaction of the modified intron 1 site sequences. (A) Sequences of modified target duplexes. The sequences shown are modified from the native APRT intron 1 site by the incorporation of a 5′-TpA or a 5′-TpApT at increasing distances from the triplex/duplex junction. The preferred 5′-TpA binding site is indicated by the underlines. (B) Photochemical reaction products observed under optimal irradiation conditions for each duplex. Duplexes 1−5 were radiolabeled on the pyrimidine-rich strand and incubated with a 20-fold excess of psorTFO1 in triplex binding buffer for 2 h at 37 °C, then subjected to irradiation for various times as described in the text, and subjected to denaturing PAGE. The gels were dried and autoradiographed and quantitated using a Betagen Betascope. The plot shows the maximum yields of total photoadducts and cross-links observed for each duplex that were obtained over the course of several separate experiments. (C) Coincident mobility of cross-linked photoadducts, phosphorylated on both duplex strands. Photoadducts of psorTFO1 and duplex 2 were prepared as described in the text, with radiolabel on the purine-rich strand, the pyrimidine-rich strand, or both strands, as indicated, and analyzed by denaturing PAGE and autoradiography. The autoradiogram on the left represents duplexes trace labeled with ^{32}P only; the autoradiogram on the right shows strands that were exhaustively labeled with nonradioactive ATP following radiolabeling (*i.e.*, both strands of each duplex contained a 5′-phosphate).

Effects on Photoadduct Formation of Insertion of 5′-TpA Sites. In order to enhance cross-link formation, duplexes were prepared containing the preferred psoralen cross-linking site (5′-TpA) at varying distances from the triplex/duplex junction (Figure 3A). All of these showed enhanced formation of total photoadducts, and some showed a dramatic enhancement of cross-link formation (Figure 3B). Formation of cross-links and monoadducts displayed a distinct distance dependence, as shown in Figure 3B. Duplex 2, with a 5′-TpA immediately adjacent to the triplex/duplex junction, gave the highest yield of photo-cross-links (>83% of total photoadducts; maximum 90%) as well as a high overall photoadduct yield (88%; maximum 90%). There was a dramatic dropoff in cross-link formation as the distance from the triplex junction to the reactive dinucleotide site increased, with almost no cross-links formed 3 bp away. In contrast, total photoadducts were formed with high efficiency with 5′-TpA even 3 bp away.

Verification of Cross-Links by Electrophoretic Mobility Comparisons. Although the bands tentatively identified above as cross-links and monoadducts have gel mobilities consistent with three-stranded and two-stranded structures, respectively, mobility alone is not conclusive, given the documented effects of sequence and branched structures on gel migration (Seeman et al., 1989). However, if the "cross-link" bands are truly cross-linked structures, then the distribution of products, as indicated by their mobilities, should be identical, regardless of which strand bears the radiolabel. When this idea was first tested, we found patterns of cross-link bands that were identical except for slightly shifted mobilities, depending on which of the complementary duplex strands was labeled (Figure 3C, left panel). To test whether the position of the 5′-phosphate on the purine-rich or pyrimidine-rich strand might cause the difference in mobility, we uniformly phosphorylated both strands with nonradioactive ATP after radiolabeling and found that the cross-link bands now migrated identically regardless of which strand was labeled (Figure 3C, right panel). This identical mobility, under conditions where isomers differing only in the 5′-phosphate position can be resolved, provides powerful evidence for cross-link formation.

Verification of Cross-Links Using a Biotinylated Target Duplex. To provide an additional test of the production of covalent cross-links, a target duplex was prepared that contained biotin on one strand and a radiolabel on the complementary strand. Following incubation with psorTFO1 and irradiation, the reaction mixture was denatured, a large excess of unlabeled single-stranded DNA identical in sequence to the labeled strand was added, and biotin-containing species were precipitated with streptavidin and biotin vesicles as described in Experimental Procedures. In the nonirradiated samples, denaturation reduced the amount of precipitated radioactivity to the low level observed with nonbiotinylated DNA, while in the irradiated samples containing putative cross-linked products, the precipitated radioactivity following denaturation remained high (Figure 4A). Autoradiography following denaturing PAGE confirmed that the precipitated radioactivity was enhanced for the slower mobility bands, identifying them as covalent cross-links of psorTFO1 and both strands of the duplex (Figure 4B). The efficiency of precipitation of radiolabel in the denatured samples, as compared to the nondenatured samples (34% *vs* 50%, or 0.68:1, Figure 4A), correlated well with the fraction of cross-links observed by PAGE (0.63:1, Figure 4B).

Specificity of PsorTFO1 Photochemical Reactions. Several control duplexes were designed to identify photoadducts and to verify the orientation of psorTFO1 binding to the target site duplex (Figure 5A). Since psoralens do not react with purine bases and react much less efficiently with C's than T's, several G·C for A·T base-pair replacements were synthesized in the target duplexes. These control duplexes were designed to address several questions about photoadduct formation in the native intron 1 site (duplex 1) as well as in the preferred site for photo-cross-links (duplex 2).

To confirm the orientation of psorTFO1 binding, a duplex target (duplex 11) was synthesized with G's in place of A's (positions 582 and 585) at the 3′ end of the pyrimidine-rich strand of duplex 2. The gel mobility and number of photoadducts did not change relative to duplex 2, indicating

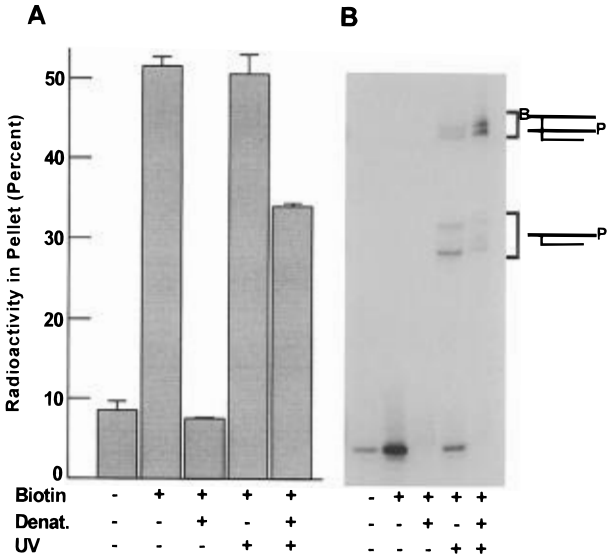

FIGURE 4: Verification of cross-links with a biotinylated duplex. (A) Radioactivity corresponding to the nonbiotinylated radiolabeled strand of the duplex target coprecipitating with its biotinylated complement, following triplex formation with psorTFO1 and indicated treatments. Denaturation (Denat.) was accomplished by heating at 97 °C for 10 min, followed by addition of a 50-fold excess of unlabeled complementary strand; UV refers to standard irradiation conditions after triplex formation as described in the text. Pelleted samples (see Experimental Procedures) were quantitated by scintillation counting and plotted as radioactivity (percent of total counts). (B) Autoradiogram of samples on a denaturing gel from an experiment parallel to that described for panel A. Deduced structures of the photoadducts are shown schematically to the right of the corresponding bands, with B referring to the biotin label and P referring to ^{32}P.

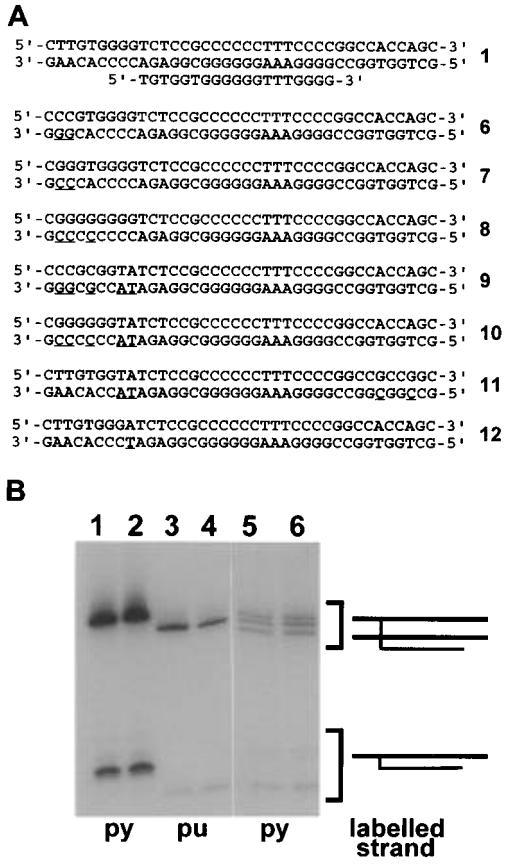

FIGURE 5: Photoreactions of psorTFO1 with duplexes designed to test specificity of photoadduct formation. (A) Sequences of duplexes tested. (B) Products of photoreaction of psorTFO1 with duplex 12 (lanes 1−4) with a 5′-ApT at the triplex junction or duplex 9 (lanes 5 and 6) with a 5′-TpApT at the triplex junction. Samples were subjected to standard irradiation conditions for 6 s, run on a denaturing 15% PAG, and then visualized by autoradiography.

that none of the photoadducts resulted from psorTFO1 reaction with T's at the 3′ end of the duplex (data not shown). This result, along with the high-efficiency cross-linking to T's at the 5′ end of the duplex (Figure 3A,B), confirms that psorTFO1 binds in the expected antiparallel orientation relative to the purine-rich strand of the target duplex.

To determine the distance restrictions on psorTFO1 photoreactions, a series of duplexes (duplex 6−duplex 10) were made by replacing T's with G's or C's, 5, 7, or 8 bases away from the triplex junction. As shown for duplex 9 in Figure 5B (lanes 5 and 6), the gel patterns remained the same (compare with Figure 3C), indicating that HMT is limited to reactions <5 bp away from the junction. This result is not surprising given that the linker length is <20 Å, which would allow reaction within a 3 bp range. A molecular model of the 38 bp target duplex with psorTFO1 bound is shown in Figure 6; the psoralen moiety is shown not intercalated to illustrate the dimensions of the photoreactive group and its linker. The structural model supports a span of HMT reaction within a 3 bp range, consistent with our results.

To confirm the role of the 5′-TpA in cross-link formation, a duplex (duplex 12) was synthesized with a 5′-ApT in place of the 5′-TpApT at the junction, reducing the number of available cross-linking sites. As shown in Figure 5B (lanes 1−4), duplex 12 shows only one band migrating as a cross-linked product as compared to the three-band pattern shown with duplex 9 (compare with lanes 5 and 6), again providing evidence for cross-link formation by psorTFO1.

Kinetics of Photoadduct Formation. In the course of determining optimal conditions for photoadduct formation, we monitored the kinetics of the photoreactions for each duplex. Figure 7A shows typical autoradiograms corresponding to time courses for duplexes 4 and 5. Figure 7B shows the results of quantitation of photoadducts as a function of time for duplexes 1−5 in an experiment in which all duplexes were treated with the same preparation of psorTFO1 under identical conditions. In each case, total photoadduct formation reached nearly its maximal extent within about 1 min; under brighter illumination the reaction was even faster, reaching completion in a few seconds (data not shown). Monoadduct formation was relatively rapid, reaching its maximal extent in about 1 min for duplexes 1, 4, and 5 and in about 6 s for duplexes 2 and 3. For duplexes 2 and 3, monoadducts likely continued to form up to 1 min but were lost to cross-links, so that the steady-state level of monoadducts remained nearly constant from 6 to 60 s. Cross-link formation, in contrast to monoadduct formation, displayed a lag in every case, presumably as a result of the delay required for sufficient monoadducts to accumulate to serve as precursors for the cross-links. Interestingly, the two duplexes that formed cross-links most efficiently (duplex 2 and duplex 3) reached their maximal cross-linking extent in about 1 min, after which the cross-links began to break down, presumably by photoreversal (see below). In contrast, duplexes 1, 4, and 5 did not display maximum cross-linking until about 10 min, and very little loss of cross-links was observed up to 30 min, possibly because of a balance between breakdown and continued slow cross-link formation.

These results can be rationalized in terms of facile intercalation at sites at or 1 bp away from the triplex/duplex

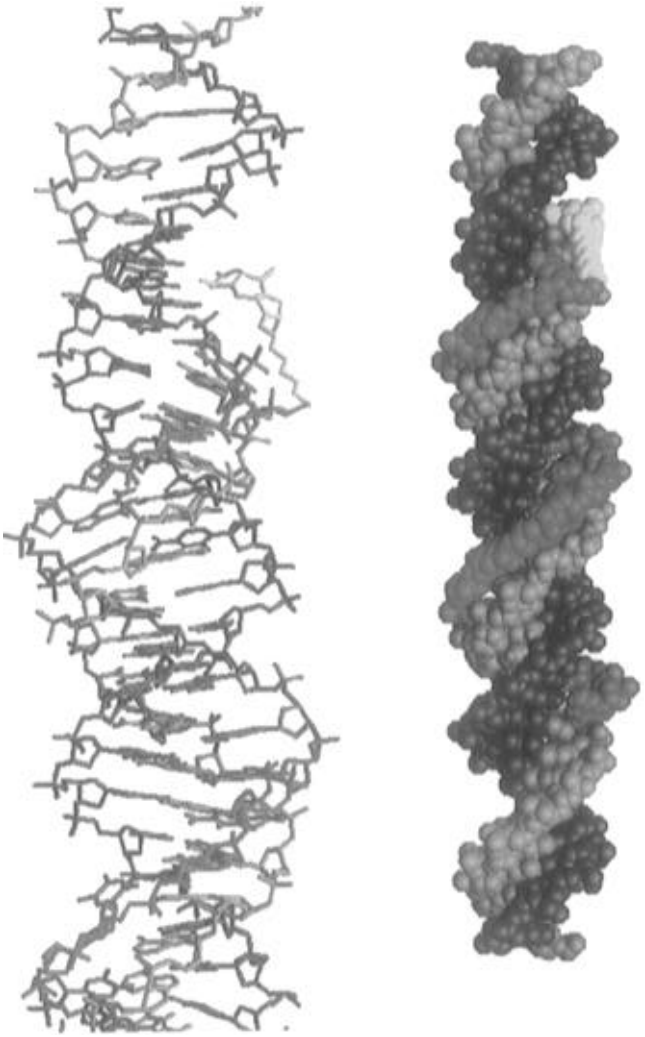

FIGURE 6: Molecular models of triplex formed by duplex 1 and psorTFO1, illustrating the geometric relationship of the psoralen moiety and the triplex junction: space-filling model (right); wire-frame model (left), enlarged to show the region of the triplex/duplex junction. The pyrimidine-rich strand of the duplex is shown in green, the purine-rich strand in blue, the TFO in red, and the psoralen moiety in yellow. The psoralen ring system is shown without intercalation to illustrate distance constraints; the photoadducts are most likely formed after intercalation. The model building with energy minimization was carried out using Biosym/MSI's Insight II molecular modeling program in a way similar to that described by Kessler et al. (1993).

junction and the well-known selective reactivity of T toward psoralen. The high yield of photoadducts observed with duplex 3 can also be attributed to its high T content near the junction, and its higher cross-linking efficiency, as compared to duplex 1, can be attributed to the presence of a nearby 5′-TpA. However, the increased distance from the junction of the 5′-TpA in duplex 3, as compared to duplex 2, appears to lower the cross-linking efficiency as shown in Figure 7B. The trend of less efficient cross-linking as the 5′-TpA was moved further from the junction continued with duplex 4 and duplex 5. Duplex 4, whose cross-linking target site was 2 bp from the junction, gave only moderate cross-link yields (15%), while moving the 5′-TpA 3 bp from the junction (duplex 5) virtually eliminated cross-linking. Both duplex 4 and duplex 5 required 10 min to reach maximum photoadduct formation, likely as a result of a requirement for rarely sampled torsionally strained conformations to achieve reaction with the more distant T residues. It is interesting that duplex 1 and duplex 5 gave comparable photoadduct yields on a similar time scale with no change in band patterns on denaturing gels, yet duplex 5 contained an extra T 3 bp away from the junction (see Figure 3A). This comparison suggests that there may be no reaction of psorTFO1 with the more distant T residue. As previously discussed, both the distribution of products and the kinetics are consistent with the length of the HMT linker.

Photoreversibility of Photoadducts. A well-known feature of covalent psoralen−DNA photoadducts is that they are fully reversible by irradiation at 240−310 nm (Cimino et al., 1986; Shi & Hearst, 1987). To confirm that the photoadducts were actually typical covalent psoralen products, we irradiated gel-purified cross-linked products at 254 nm. Figure 8 shows that the cross-linked products were fully reversible (compare lanes 2 and 3), consistent with covalent HMT−DNA photoadducts.

If the gel-purified products had been covalent furan-sided monoadducts, instead of cross-links, then upon a second irradiation at 334 nm, cross-links would have been expected to result. As shown in Figure 8, the mobility of the gel-purified products was identical with that of the product resulting from a second round of irradiation at 334 nm (compare lanes 2 and 4). This result also supports our conclusion that the initial products were covalent HMT−DNA cross-links.

DISCUSSION

Triplex technology offers an alternative approach to genome manipulation that could overcome a number of limitations to the currently available methodology: unknown biological consequences of using viral vectors, mutations associated with random integration, and low frequencies of targeted recombination. These studies were designed to test the feasibility of using triplex-mediated photochemistry as a key element in a gene manipulation strategy that would allow targeting of specific sites within any gene with high efficiency, followed by controlled activation of the gene modification process. Triplex technology potentially offers a number of important advantages: high-affinity binding directed at only one or two targets per cell, direct inactivation of a gene, and sensitization of a gene for targeted recombination. Photochemically damaging DNA at a specific site should enhance the rate of recombination at that site and, therefore, increase the efficiency of gene therapeutics. Psoralen activation by UVA may be particularly useful for studies in cultured cells and for treatment of accessible tissues. However, visible light activation of psoralen (Gasparro et al., 1993) may allow deeper tissue penetration and may be less mutagenic than UVA.

PsorTFO1 Binding to the Native APRT Intron 1 Site. We have shown here that a psoralen-modified TFO (psorTFO1) forms triplex with high affinity by binding the underlying duplex in an antiparallel fashion. Surprisingly, the psoralen modification does not appear to enhance binding affinity, in contrast to other studies with intercalator-modified TFOs (Le Doan et al., 1987; Grigoriev et al., 1992; Mouscadet et al., 1994).

Cross-Links vs Monoadducts. Although the effects on chromosomal recombination and mutation of triplex-mediated photoreactions will have to be determined by experiments in living cells, there is already considerable information about the effects of psoralen monoadducts and cross-links on recombination and mutation in mammalian cells.

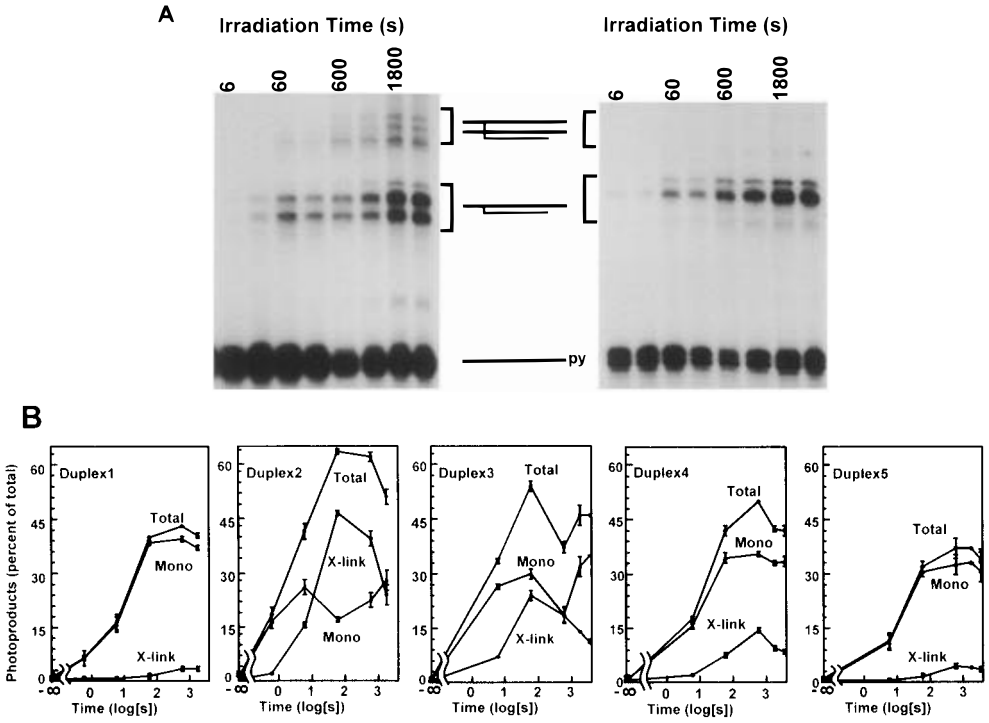

FIGURE 7: Kinetics of photoadduct formation. (A) Time courses of photoadduct formation for duplexes 4 and 5. Following incubation of psorTFO1 with 5′-end-labeled duplex, the samples were incubated for 0−60 min, and then products were separated by denaturing gel electrophoresis on a 15% polyacrylamide gel and subjected to autoradiography. (B) Similar samples were prepared for duplexes 1−5, and the radioactivity was quantitated using a Betagen Betascope. The results are plotted as a percent of the total radioactivity in cross-linked adducts (X-link), monoadducts (Mono), or their sum (Total) *vs* irradiation time. Time is plotted on a log scale to show the full range of kinetic behavior observed.

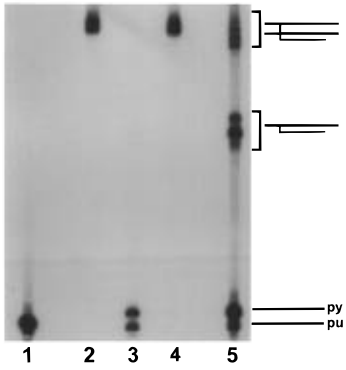

FIGURE 8: Photoreversibilty of photoadducts. Following standard incubation and irradiation procedures for duplex 2, the photoadducts were separated by PAGE on a 15%, 7 M urea gel buffered with TBE. After irradiation cross-linked bands were gel purified and then irradiated a second time with UV of either 254 or 334 nm and then again subjected to PAGE, along with control samples. Lane 1 contains a control reaction mixture that was not subjected to the initial irradiation; lane 2 contains the gel-purified photo-cross-linked products without a second irradiation; lane 3 contains the same sample as in lane 2 after a second irradiation at 254 nm; lane 4 contains the same sample as in lane 2 after a second irradiation at 334 nm; lane 5 contains the irradiated mixture from which the cross-linked species in lane 2 was purified.

The relatively greater potency of cross-links in stimulating these processes has been tied to the mechanisms by which they are repaired (Sladek et al., 1989; Cheng et al., 1988). It can be argued that monoadducts are also mutagenic as they have been implicated in enhancing the frequency of mutation in mammalian cells (Gunther et al., 1995). Thus, establishing the sequence requirements for efficient formation of both monoadducts and cross-links is essential for analyzing the *in vivo* effects of these photoadducts. The results described here make it clear that the distance of 5′-TpA sites from the triplex/duplex junction is the most important determinant of both the efficiency of product formation and the proportions of monoadducts and cross-links. This sensitivity to position might be expected since the conformation of the triplex/duplex junction differs from either B-form duplex DNA or A-form triplex DNA (Radhakrishnan & Patel, 1994). The triplex/duplex junction has been shown to be more reactive to intercalating agents (Collier et al., 1991; Sun et al., 1991), and therefore, it might be expected that psoralen would have greater potential for reaction at the junction. In fact, for psoralen-linked triplexes, simple considerations of linker length, sequence, and sequence context (*i.e.*, proximity to the triplex/duplex junction) can be used to estimate the outcome fairly accurately.

Photoreaction Kinetics. Additional features of the photoreactions with great significance for intracellular applications are the dependence on time and radiation dose. Obviously, a requirement for prolonged irradiation with UV light would preclude studies in viable cells. Our results show that the ultimate yield of photoadducts after irradiation is dependent on sequence with a 5′-TpApT being favored for formation of cross-links and an overall high yield of photoadducts. The distance of T's from the triplex/duplex junction is critical in the formation of both cross-links and monoadducts. The kinetics of photoadduct formation imply, as expected, that there is an initial increase in monoadduct formation with a subsequent increase in cross-links. It also appears that the further the 5′-TpA is from the junction, the more time required for cross-link formation (see Figure 7).

Implications for Gene Targeting. The efficiency of psoralen photoadduct formation at the native intron 1 site (∼50%) is encouraging, although it appears that the products are predominantly the result of psorTFO1 covalently cross-linking to one strand of the target duplex, and not both. The

inability of psorTFO1 to cross-link to both strands of the target duplex was not unexpected: the target site contains a 5′-GpT at the triplex junction, a sequence that does not form photo-cross-links efficiently with psoralen. A comparison of the effects of monoadducts *vs* cross-links on chromosomal recombination seems a requirement for maximizing the use of site-specific DNA damage as a tool for precise genome manipulation. We are currently testing the effects of monoadduct formation on recombination and mutation frequencies in cells using the native APRT intron 1 site in CHO cells.

Perhaps the most important conclusion for immediate application of triplex-mediated psoralen photochemistry to genome manipulation in living cells is that the sequence immediately adjacent to the triplex binding site in the target duplex is critically important. Specifically, at least one thymine residue must be within reach of the psoralen for efficient photoadduct formation, and rapid and efficient photo-cross-linking requires a 5′-TpA sequence immediately adjacent to the triplex/duplex junction. Because duplex 2 shows very high efficiency cross-link formation, this sequence is a promising site to target into the APRT gene in CHO cells to test its effect on recombination and mutation. We are currently testing the applicability of these now well-defined *in vitro* rules, to the conditions present in the nuclei of mammalian cells, using modified APRT genes engineered into hamster chromosomes.

ACKNOWLEDGMENT

We thank Dr. Veeraiah Bodepudi and Robert Tinder for preparing psorTFO1, Sean Smith for the molecular modeling studies of the psorTFO1 triplex, and Mark Brenneman, April Kilburn, Kathleen Marburger, Ray Merrihew, and Geoff Sargent for helpful discussions.

REFERENCES

Averbeck, D. (1985) *Mutat. Res. 151*, 217−233.
Beal, P. A., & Dervan, P. B. (1991) *Science 251*, 1360−1363.
Ben-Hur, E., & Song, P. S. (1984) *Adv. Radiat. Biol. 11*, 131−157.
Birg, F., Praseuth D., Zerial, A., Thuong, N. T., Asseline, U., LeDoan, T., & Helene, C. (1990) *Nucleic Acids Res. 18*, 2901−2908.
Bridges, B. A., Mottershead, R. P., & Knowles, A. (1979) *Chem.-Biol. Interact. 27*, 221−233.
Cheng, S., Van Houten, B., Gamper, H. B., Sancar, A., & Hearst, J. E. (1988) *J. Biol. Chem. 263*, 15110−15117.
Cimino, G. D., Gamper, H. B., Isaacs, S. T., & Hearst, J. E. (1985) *Annu. Rev. Biochem. 54*, 1151−1193.
Cimino, G. D., Shi, Y., & Hearst, J. E. (1986) *Biochemistry 25*, 3013−3020.
Cole, R. S. (1971) *Biochim. Biophys. Acta 254*, 30−39.
Colier, D. A., Mergny, J. L., Thuong, N. T., & Helene, C. (1991) *Nucleic Acids Res. 19*, 4219−24.
Cooney, M., Czernuszewicz, G., Postel, E. H., Flint, S. J., & Hogan, M. E. (1988) *Science 241*, 456−459.
Degols, G., Clarenc, J. P., Lebleu, B., & Leonetti, J. P. (1994) *J. Biol. Chem. 269*, 16933−16937.
Esposito, F., Brankamp, R. G., & Sinden, R. R. (1988) *J. Biol. Chem. 263*, 11466−11472.
Friedberg, E. C., Walker, G. C., & Siede, W. (1995) *DNA Repair and Mutagenesis*, pp 523−576, ASM Press, Washington DC.
Gasparro, F. P., Gattolin, P., & Olack, G. A. (1993) *Photochem. Photobiol. 57*, 1007−1010.
Gasparro, F. P., Havre, P. A., Olack, G. A., Gunther, E. J., & Glazer, P. M. (1994) *Nucleic Acids Res. 22*, 2845−2852.
Grigoriev, M., Praseuth, D., Robin, P., Hemar, A., Saison-Behmoaras, T., Dautry-Varsat, A., Thuong, N. T., Helene, C., & Harel-Bellan, A. (1992) *J. Biol. Chem. 267*, 3389−3395.
Grigoriev, M., Praseuth, D., Guieysse, A. L., Robin, P., Thuong, N. T., Helene, C., & Harel-Bellan, A. (1993) *Proc. Natl. Acad. Sci. U.S.A. 90*, 3501−3505.
Gunther, E. J., Yeasky, T. M., Gasparro, F. P., & Glazer, P. M. (1995) *Cancer Res. 55*, 1283−1288.
Hall, J. D. (1982) *Mol. Gen. Genet. 188*, 135−138.
Havre, P. A., & Glazer, P. M. (1993) *J. Virol. 67*, 7324−7331.
Havre, P. A., Gunther, E. J., Gasparro, F. P., & Glazer, P. M. (1993) *Proc. Natl. Acad. Sci. U.S.A. 90*, 7879−7883.
Ing, N. H., Beekman, J. M., Kessler, D. J., Murphy, M., Jayaraman, K., Zendegui, J. G., Hogan, M. E., O'Malley, B. W., & Tsai, M. (1993) *Nucleic Acids Res. 21*, 2789−2796.
Kessler, D. J., Pettitt, B. M., Cheng, Y.-K., Smith, S. R., Jayaraman, K., Vu, H. M., & Hogan, M. E. (1993) *Nucleic Acids Res. 21*, 4810−4815.
Kovacs, A., Kandala, J. C., Weber, K. T., & Guntaka, R. V. (1996) *J. Biol. Chem. 271*, 1805−1812.
Le Doan, T., Perrouault, L., Praseuth, D., Habhoub, N., Decout, J. L., Thuong, N. T., Lhomme, J., & Helene, C. (1987) *Nucleic Acids Res. 15*, 7749−7760.
McShan, W. M., Rossen, R. D., Laughter, A. H., Trial, J., Kessler, D. J., Zendegui, J. G., Hogan, M. E., & Orson, F. M. (1992) *J. Biol. Chem. 267*, 5712−5721.
Moser, H. E., & Dervan, P. B. (1987) *Science 238*, 645−650.
Mouscadet, J. F., Ketterle, C., Goulaouic, H., Carteau, S., Subra, F., Le Bret, M., & Auclair, C. (1994) *Biochemistry 33*, 4187−4196.
Okada, T., Yamaguchi, K., & Yamashita, Y. (1994) *Growth Factors 11*, 259−270.
Orson, F. M., Thomas, D. W., McShan, W. M., Kessler, D. J., & Hogan, M. E. (1991) *Nucleic Acids Res. 19*, 3435−3441.
Perrouault, L., Asseline, U., Rivalle, C., Thuong, N. T., Bisagni, E., Giovannangeli, C., Le Doan, T., & Helene, C. (1990) *Nature 344*, 358−360.
Postel, E. H., Flint, S. J., Kessler, D. J., & Hogan, M. E. (1991) *Proc. Natl. Acad. Sci. U.S.A. 88*, 8227−8231.
Radhakrishnan, I., & Patel, D. J. (1994) *Biochemistry 33*, 11405−11416.
Reardon, J. T. R., Spielman, P., Huang, J. C., Sastry, S., Sancar, A., & Hearst, J. E. (1991) *Nucleic Acids Res. 19*, 4623−4629.
Roy, C. (1994) *Eur. J. Biochem. 220*, 493−503.
Sargent, R. G., Merrihew, R. V., Nairn, R., Adair, G., Meuth, M., & Wilson, J. H. (1996) *Nucleic Acids Res. 24*, 746−753.
Scaggiante, B., Morassutti, C., Tolazzi, G., Michelutti, A., Baccarani, M., & Quadrifoglio, F. (1994) *FEBS Lett. 352*, 380−384.
Seeman, N. C., Chen, J. H., & Kallenbach, N. R. (1989) *Electrophoresis 10*, 345−354.
Shi, Y., & Hearst, J. E. (1987) *Biochemistry 26*, 3786−3792.
Sladek, F. M., Melian, A., & Howard-Flanders, P. (1989) *Proc. Natl. Acad. Sci. U.S.A. 86*, 3982−3986.
Sun, J. S., Lavery, R., Chomilier, J., Zakrzewska, K., Montenay-Garstier, T., & Helene, C. (1991) *J. Biomol. Struct. Dyn. 9*, 425−436.
Takasugi, M., Guendouz, A., Chassignol, M., Decout, J. L., Lhomme, J., Thuong, N. T., & Helene, C. (1991) *Proc. Natl. Acad. Sci. U.S.A. 88*, 5602−5606.
Tu, G. C., Cao, Q. N., & Israel, Y. (1995) *J. Biol. Chem. 270*, 28402−28407.
Vasquez, K. M., Wensel, T. G., Hogan, M. E., & Wilson, J. H. (1995) *Biochemistry 34*, 7243−251.
Wang, G., Levy, D. D., Seidman, M. M., & Glazer, P. M. (1995) *Mol. Cell. Biol. 15*, 1759−1768.
Wang, G., Levy, D. D., Seidman, M. M., & Glazer, P. M. (1996) *Science 271*, 802−805.
Zendegui, J. G., Vasquez, K. M., Tinsley, J. H., Kessler, D. J., & Hogan, M. E. (1992) *Nucleic Acids Res. 20*, 307−314.

BI960881F